Biomedical Technology 6 (2024) 1–8

Contents lists available at ScienceDirect

Biomedical Technology

journal homepage: www.keaipublishing.com/en/journals/biomedical-technology

Research Paper

A computational model to assess the effectiveness of adhesive materials in restoration of crown-root fractures

Amandeep Kaur [a,1], Shubham Gupta [b,1], Nitesh Tewari [c], Arnab Chanda [b,d,*]

[a] Department of Conservative Dentistry and Endodontics, Regional Institute of Medical Sciences, Manipur, India
[b] Centre for Biomedical Engineering, Indian Institute of Technology (IIT), Delhi, India
[c] Department of Paedodontics and Preventive Dentistry, All India Institute of Medical Sciences(AIIMS), Delhi, India
[d] Department of Biomedical Engineering, All India Institute of Medical Sciences (AIIMS), Delhi, India

ARTICLE INFO

Keywords:
Dental trauma
Crown-root fracture
Fragment Re-Attachment
Adhesive
Finite element analysis

ABSTRACT

Fragment reattachment for crown root fractures has become a routinely employed treatment modality with the advancements in adhesive dentistry. Among the majority of documented dental trauma cases, this specific fracture type is one of the most prevalent and difficult fracture kinds. Due to its complexity, these fracture kinds are often not computationally modelled. Moreover, there is a lack of literature to understand the effect of different adhesive materials, used to re-attach this particular fracture, on traumatic injuries. In our work, 3D models of the permanent maxillary central incisor tooth were developed using cone beam computed tomography image of a patient. This model was systematically modified to represent a prominent crown root fracture and subsequently re-attached computationally using three different adhesives. A biting force and a traumatic load were applied, and the induced stresses were studied across the healthy and treated tooth models and compared for three different adhesives used for re-attachment of fractured fragments. Tooth reattached with resin adhesive performed better in all the loading conditions that were considered in the study as compared to flowable composite and resin cement.

1. Introduction

Crown-root fractures involving enamel, dentine and cementum are commonly encountered injuries in children and adolescents accounting for 5% of all traumatic dental injuries (TDIs) [1]. They are classified as uncomplicated when no pulp exposure is present and complicated when pulp exposure is evident [2]. When the fractured fragment is available with no or minimal violation of the biologic width, reattachment is a viable treatment option [3]. Autogenous fragment reattachment to the fractured tooth remains the treatment of choice due to its simplicity, esthetics, conservation of tooth structure and cost-effectiveness [4]. Additionally, life-like translucency is achieved and incisal edge wear is similar to adjacent teeth with positive psychological effect [5]. A systematic review by Khandelwal et al. [6] concluded that fragment reattachment after complicated crown root fractures can be considered as a viable treatment option when clinical conditions are favourable.

Functional and esthetic success has been reported with the use of adhesive luting systems and dentine bonding agents [7]. The effectiveness of the adhesive system and the intermediate materials used to bond the fractured segment to the remaining tooth plays a pivotal role in the longevity of the coronal fragment reattached. The loss of reattached fragment may occur due to non-physiological use of the restored tooth or new trauma. Therefore, fracture strength of the restored tooth is a pertinent and frequent concern.

Finite element analysis (FEA) is a convenient and appropriate method [8,9] to assess the stresses and strains generated in complex structures under different loading conditions using computational models. In a previous work by Garg et al. [10], two dental fractures were considered and computationally tested using different adhesive materials. It consisted of a fixed fracture angle of 60° which resulted majorly in a root fracture (and not crown-root fracture). Whereas, the current work considered a more prominent crown-root fracture extending from the incisal edge of the crown to cervical-third of the root. This particular fracture is highly common and one of the most challenging fracture types amongst the majority of reported dental trauma cases [11,12]. In another recent FEA study, Wang et al. [13], studied the fracture resistance of a

* Corresponding author. All India Institute of Medical Sciences (AIIMS), Delhi, India.
E-mail addresses: amandoc24@gmail.com (A. Kaur), Shubham.Gupta@cbme.iitd.ac.in (S. Gupta), dr.nitesht@gmail.com (N. Tewari), arnab.chanda@cbme.iitd.ac.in (A. Chanda).
[1] Both the Authors have contributed equally.

https://doi.org/10.1016/j.bmt.2023.09.002
Received 1 June 2023; Received in revised form 4 September 2023; Accepted 14 September 2023

mandibular first molar having complex cavities. The study found that contracted endodontic cavity showed better resistance to fractures. In a recent work by Rathod et al. [14], computational investigation was done to study the stress distribution of zygomatic implants in maxillectomy cases. The study reported maximum and minimum stresses at the distal head and apex of the implant respectively. Sender et al. [15], studied the biomechanics of tooth strength using a FE model. Crown was found to have the highest risk of fracture due to hard object biting.

This is of particular importance for investigating inaccessible anatomical sites *in vivo* and traumatic events which cannot be tested in situ thereby predicting potential areas of structural failure [16,17]. Low cost and high reliability are added advantages of FEA studies [18]. Furthermore, this method provides an insight into the response of biological tissues affected by biomechanical events [19]. Therefore, the aim of this study was to evaluate deformation and stresses generated during a new trauma in a permanent maxillary incisor tooth where fragment re-attachment was done previously with different adhesive materials. The null hypothesis tested was that the stresses and strains generated during the traumatic loading would not affect the already treated tooth.

2. Materials and methods

2.1. Geometrical model

Three-dimensional (3D) data acquisition technique produces accurate geometry with increased accuracy in results [20,21]. In our work, a 3D reconstructed model of a removed tooth was developed from cone beam computed tomography (CBCT) scans from an 18-year-old male. CBCT images were taken with a CS 9300 scanner (Care stream Health Inc., Rochester, NY, USA) with pulsed exposure, voxel size of 300 × 300 × 300μm, field of view (FOV) 130 mm, exposure parameters of 80 KVp, 10 Ma in a 360-degree rotation and 11 s exposure time. The CBCT data was exported in Digital Imaging and Communication in Medicine (DICOM) file format and imported into a medical software (Mimics 18.0, Materialise Dental, Leuven, Belgium). The segmentation of various structures including enamel, dentin, pulp and cementum was done using image density thresholding. Penetrations between surfaces were carefully avoided through precision contouring technique. The 3D triangle-based surface of each structure of permanent maxillary incisor tooth obtained after segmentation was exported in Stereo Lithography (STL) format. Fig. 1A shows various parts of the scanned tooth model. The dimensions are in line with the permanent maxillary central incisor tooth (total length from incisal edge to root apex: 23.50 mm, root length from cemento-enamel junction to root apex: 13.70 mm) [22]. For the reattached tooth model, Dassault Systèmes SolidWorks 2017 (Vélizy-Villacoublay, France) was employed, and a crown-root fracture was considered with the fracture line extending from the incisal edge of the crown to cervical-third of the root (Fig. 1B). A part in the model adjacent to the fracture line having a thickness of 25 μm was cut and another part geometry was extruded to fill the gap that was earlier cut and was provided with the filler material properties (Fig. 1C).

2.2. Material model

Specific properties of each material of the tooth model, and the three adhesive variants, including their Young's modulus (E) and Poisson's ratio (v) were employed in the computational model (Table 1) (Huang et al.) [23]. As all the adhesive materials are commonly available for application, it was assumed that they were all biocompatible (as per International standard ISO 7405 entitled for the preclinical evaluation of bio-compatibility of medical devices used in dentistry and test methods for dental materials). Minor anisotropic effects due to non-linearity were not considered. The thickness of the adhesive system (flowable composite, resin cement and resin adhesive) was taken as per ISO standards for luting cements as 25 μm for standardization [24].

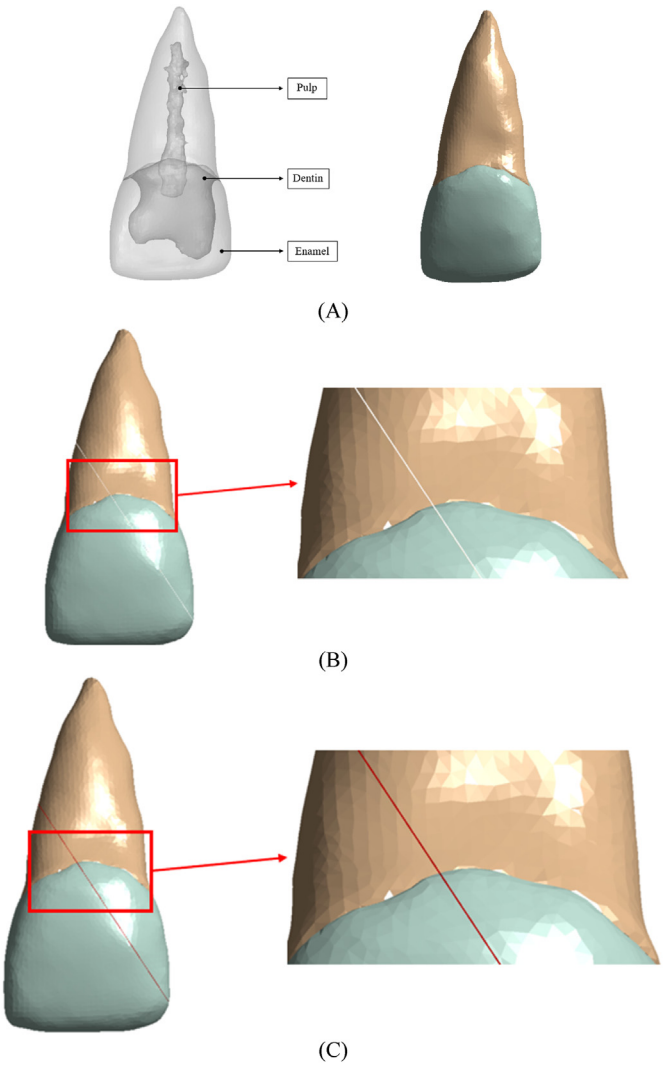

Fig. 1. Geometrical model of the: A) Tooth with its parts, B) Cut operation simulating a crown-root fracture, and C) Added filler material for reattachment.

Table 1
Material Properties of tooth parts and adhesives.

Material properties	Young's modulus (GPa)	Poisson's ratio
Enamel	77.90	0.30
Dentin	16.60	0.30
Pulp	6.89E-3	0.45
Flowable composite (Filtek P60)	19.70	0.32
Resin cement (RelyX ARC)	4.92	0.27
Resin adhesive	1.00	0.24

2.3. Finite element (FE) model

Effective FE modelling involves discretization of the geometries and subsequently generation of a computationally viable mesh and assignment of loads and boundary conditions. The finite element models (FEM) were generated using ANSYS Workbench 19 R2 (Ansys, Inc., Canonsburg, Pennsylvania, USA).

In the FEM, the physics preference for each model was set as 'mechanical' as the considered material models were linear and isotropic. In addition to this, an adaptive sizing method with a resolution of value '2' was applied to enhance the overall accuracy of the mesh. For refinement at the areas of loading, mesh defeaturing along with a fine span centre angle was applied. Optimal computational meshes were generated using

a combination of linear tetrahedral elements with smooth transition ratio of 0.27 and element sizes ranging from 0.2 mm to 0.6 mm depending upon geometry (Fig. 2A). Other parameters such as maximum layers and growth rate of the meshes were set as '5' and '1.2' respectively. For the tooth models, a contact pair with characteristics as 'bonded' (using flexible and always bonded type contact pairs) was employed without considering small sliding of elements. A trim tolerance of 0.0008 mm was applied between enamel, dentin and pulp. Each element was characterized with 20-node Solid 186 as these element type ensures accuracy of results in large deformations and complex contact conditions [25–27].

A detailed mesh sensitivity analysis (Fig. 2) was conducted to select the optimal mesh. Both the tooth models were meshed with six different incremental meshes. Healthy tooth model was meshed with six different meshes, namely default (10420 elements), very coarse (25648 elements), coarse (40235 elements), fine (64810 elements), very fine (90345 elements), and finest (105462 elements) models (Fig. 2A). Whereas, reattached tooth model was meshed with default (12465 elements), very coarse (27689 elements), coarse (45631 elements), fine (86434 elements), very fine (98764 elements), and finest (110345 elements) models (Fig. 2B). The mesh which produced low variations (i.e., below 5%) in the result was selected as the optimal mesh size. As a result, for healthy and reattached tooth, mesh elements of 64810 and 86434 was selected and used throughout the study.

The enamel model was generated with 22278 elements, dentin with 36147 and pulp with 6385 elements. Cementum was not modelled because of small thickness and physical properties similar to dentin. The reattached tooth model was generated with 86434 elements (Fig. 3A). Two types of loads and boundary conditions were applied. To simulate the realistic dental biomechanics, the entire root surface was constrained in all degrees of freedom and pressure equivalent to a force of 33 N was applied to simulate normal masticatory load on the incisal edge of the crown of the normal and the reattached tooth (Fig. 3B). Additionally, to simulate a traumatic load, pressure equivalent to a force of 2000 N with a time period of 1 s was applied on the centre of the labial surface of the reattached tooth at 90° to the cleidocranial direction (Fig. 3B). This was done since frontal and incisal traumas are the most common [28].

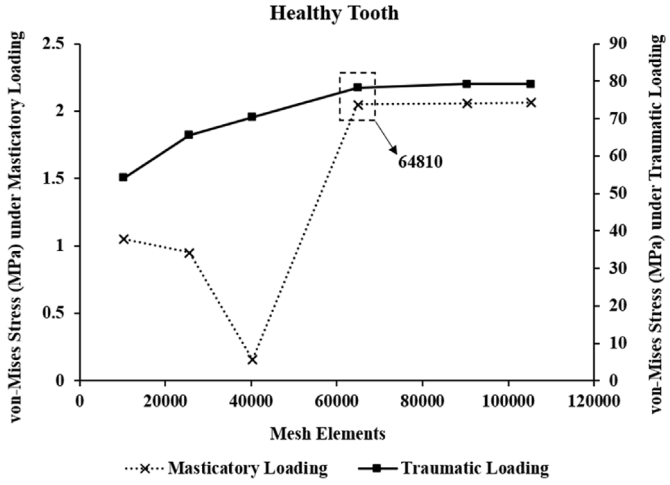

Fig. 2. Mesh sensitivity test for (A) Healthy tooth, and (B) Reattached tooth.

3. Results

The maximum stress, strain, displacements in the X, Y, and Z directions, and the net displacement vector sum were evaluated. The results obtained were quantified using von- Mises stress and shear stress index. The results are presented in linear and logarithmic color scales where each color corresponds to the deformation or stress value intervals in mm and MPa respectively.

3.1. Deformation and stress distribution in normal tooth

Fig. 4A shows the total deformation in a normal tooth as a result of a masticatory load. The maximum deformation estimated was 0.00116 mm and observed at the incisal edge which decreased towards the cervical area of the crown, and was minimum at the root surface. The maximum von-Mises stress recorded was 2.05 MPa (Fig. 4B) along the cemento-enamel junction (CEJ). The minimum von-Mises stress values were

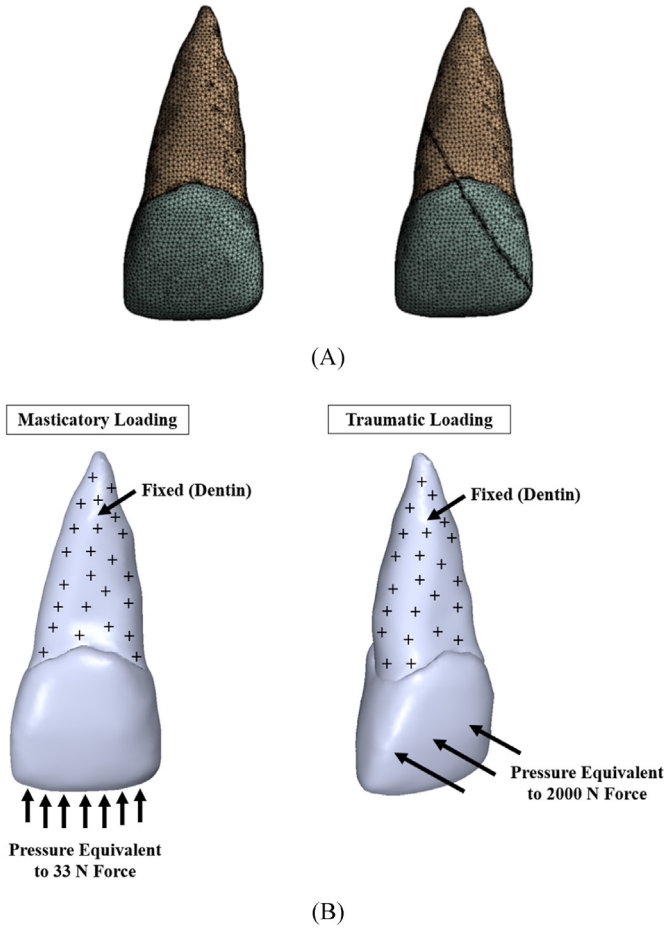

Fig. 3. A) Meshes of the healthy and reattached tooth models, B) Boundary conditions.

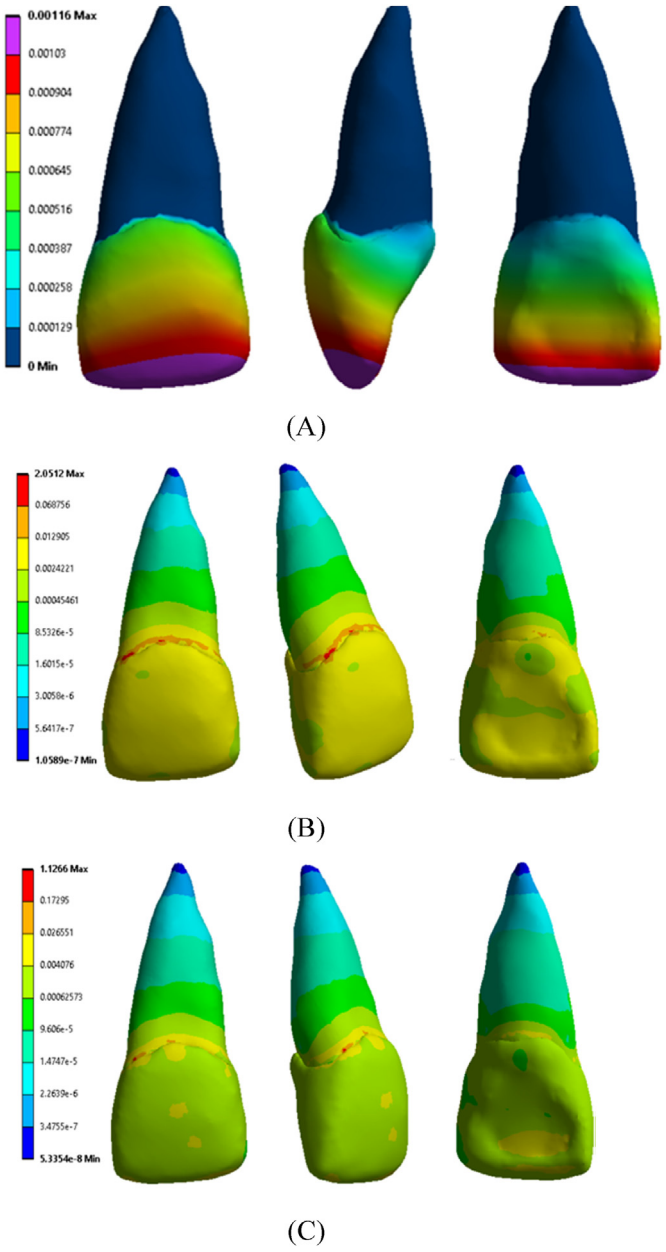

Fig. 4. Different views of the healthy tooth model: A) Total deformation, B) von-Mises stresses, C) Shear stresses.

found at the root apex. Furthermore, the maximum shear stress was observed along the CEJ whereas minimum shear stress values were recorded at the root apex. The entire crown surface, the cervical-third and middle-third demonstrated moderate to low shear stress values.

3.2. Deformation and stress distribution in reattached tooth under varying loads

3.2.1. Masticatory load

The maximum deformation in the tooth re-attached with flowable composite as a result of masticatory load (33 N) was 0.0011 mm, which was observed along the incisal edge of the crown. The deformation decreased from middle-third to gingival-third of the crown and was the least along the entire length of the root surface (Fig. 5A). Maximum von-Mises stress of 21.37 MPa was induced along the fracture line where re-attachment had been done with flowable composite. The lowest von Misses stress was recorded at the tip of the root. Moderate stresses were observed in the crown portion of the tooth which decreased along the root (Fig. 5B). Maximum shear stress of 11.92 MPa was estimated along the fracture line in the cervical-third of the root. High shear stress was seen around CEJ. Low shear stresses were observed in the crown portion of the tooth and cervical-third and middle-third of the root. Minimum shear stress was quantified in the apical-third of the root (Fig. 5C).

The maximum deformation in the tooth re-attached with resin cement as a result of masticatory load was 0.00131 mm along the incisal edge (Fig. 6A). The deformation declined from incisal-third to cervical-third of the crown. The root surface from cervical-third to apical-third depicted minimum deformation. Maximum von-Mises stress of 15.15 MPa was recorded at the CEJ and the fracture line in the cervical-third of the root (Fig. 6B). von-Mises stress of 0.12 MPa was estimated on the labial surface of the crown in the cervical and middle part along with the CEJ. The stress declined going from the crown of the tooth to the root, and exhibited the minimum value at the root tip. Maximum shear stress of 8.31 MPa was observed in the CEJ region and cervical-third of the root along the length of the fracture line (Fig. 6C). High shear stress was evident on the labial surface of the tooth crown. It decreased in the root with its minimum at the root tip.

A trend similar to that in the case of resin cement, was observed for the resin adhesive, in response to the masticatory load on the reattached tooth model. Maximum deformation of 0.00153 mm (Fig. 7A) was estimated on the incisal edge and incisal-third of the tooth crown. The deformation decreased towards the root. Maximum von-Mises stress of 7.33 MPa (Fig. 7B) was seen at the CEJ extending to the fracture line in the cervical-third of the root. Labial surface of the crown and the CEJ were also found to have high stress concentrations. Minimum stress was observed at the root tip. Likewise, maximum shear stress of 3.92 MPa (Fig. 7C) was found along the CEJ and fracture line in cervical-third of root. High to moderate shear stresses were present in the crown and

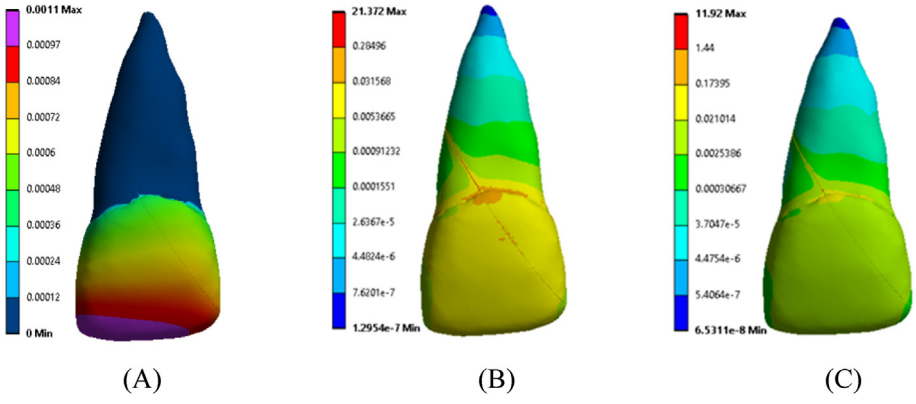

Fig. 5. Tooth model with flowable composite reattachment, under masticatory load: A) Total deformation, B) von-Mises stresses, C) Shear stresses.

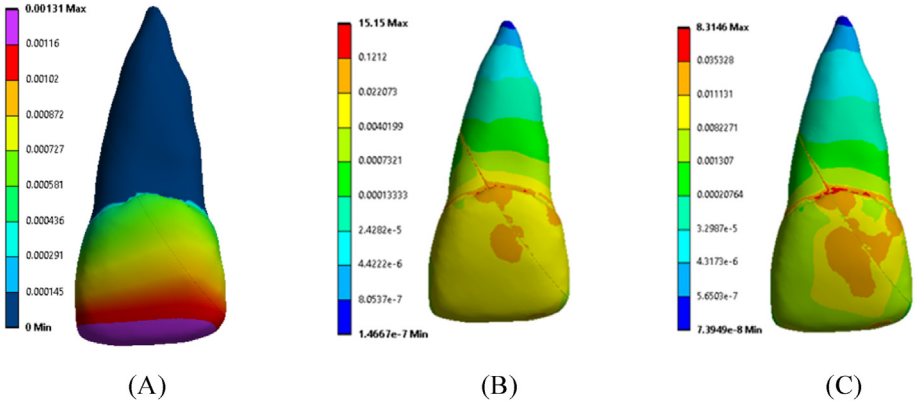

Fig. 6. Tooth model with resin cement reattachment, under masticatory load: A) Total deformation, B) von-Mises stresses, C) Shear stresses.

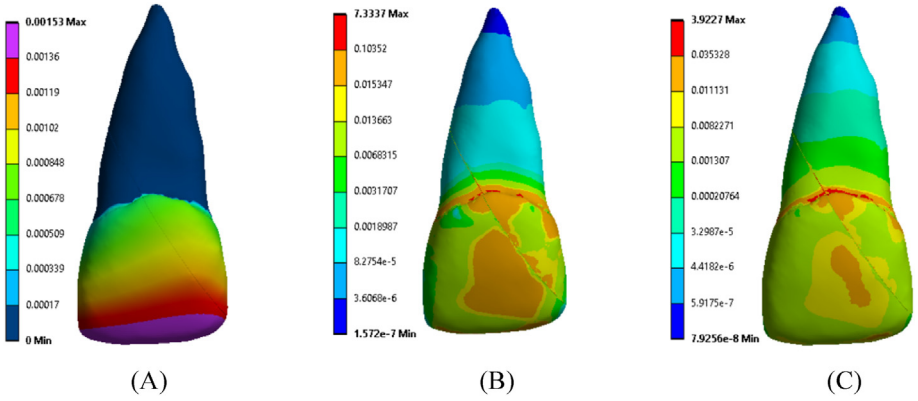

Fig. 7. Tooth model with resin adhesive reattachment, under masticatory load: A) Total deformation, B) von-Mises stresses, C) Shear stresses.

cervical-third of the root. The shear stress dropped in apical-third of the root with its minimum at the root tip.

3.2.2. *Traumatic load*

The maximum deformation in a healthy maxillary central incisor tooth as a result of a traumatic force (2000 N) was 0.0753 mm at the incisal edge of the crown (Fig. 8A). Root surface demonstrated minimum deformation. Maximum von-Mises stress of 78.20 MPa was observed in the crown and CEJ, and minimum at the root tip. Maximum shear stress was 40.94 MPa at the CEJ. High shear stress was estimated in the crown portion, followed by moderate in the cervical and middle-third of the root, and least in the apical-third of the root.

Maximum deformation in the tooth reattached with flowable composite as a result of a traumatic load was 0.0198 mm at the incisal edge

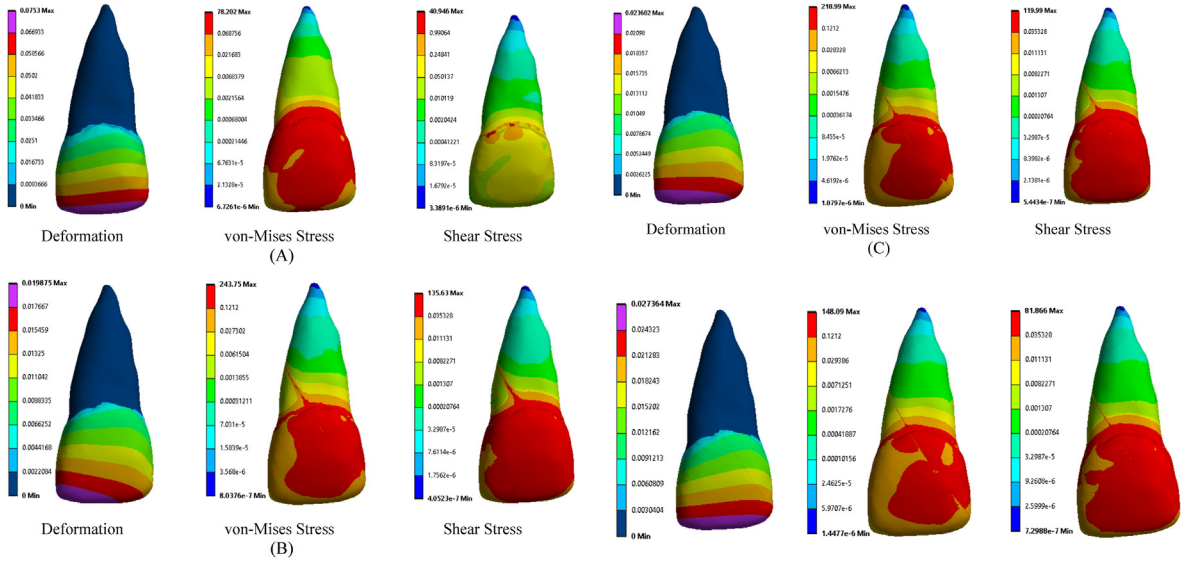

Fig. 8. Total deformation, von-Mises stresses, and shear stresses observed due to application of traumatic load in A) Healthy tooth, and reattached tooth models with B) Flowable composite, C) Resin cement, and D) Resin adhesive.

with minimum deformation along the root (Fig. 8B). Maximum von-Mises stress of 243.75 MPa was observed in the crown and CEJ region. High stress was observed in the cervical-third of the root, which decreased apically with its minimum at the tip of the root. Maximum shear stress of 135.63 MPa was also recorded in the crown and CEJ region, which reduced in the root and was the least at the root tip.

The maximum deformation in the tooth reattached with resin cement as a result of a traumatic load was 0.0236 mm at the incisal edge (Fig. 8C). The root depicted minimum deformation. Maximum von-Mises stress of 218.99 MPa was observed in the crown, CEJ region and along the fracture line. It gradually dropped along the length of the root apically. Similarly, the maximum shear stress of 119.99 MPa was evident in the crown, CEJ and the fracture line. It declined apically in the root.

When the traumatic force was applied to the tooth reattached with resin adhesive, maximum deformation of 0.273 mm was estimated in the incisal area of the crown and minimum deformation at the constrained root (Fig. 8D). Maximum von-Mises stress was observed in the crown, CEJ, and the fracture line, which decreased in the root portion. Similar trend was observed with the shear stress. Maximum shear stress was quantified in the crown, CEJ, and fracture line. The shear stress decreased from the crown towards the root and was minimum at the root tip.

3.2.3. Comparison across tooth condition and loads

Under masticatory loading, von-Mises stress as low as 0.36 MPa was generated in the enamel (Fig. 9). This significantly increased for the reattached tooth model. The highest stresses were recorded with the flowable composite (21.37 MPa) based reattachment, followed by the resin cement (15.15 MPa) and resin adhesive (7.33 MPa). For the dentin, the reattached tooth models developed slightly lower von-Mises stress in the range of 1–1.50 MPa compared to that of the healthy tooth (2.05 MPa). Overall, the stresses developed at the dentin were significantly lower than that of the enamel.

On application of the traumatic load, the enamel and dentin developed similar maximum stresses in the healthy tooth model (Fig. 10). With the tooth reattachment, a similar trend was observed. However, the magnitude of these stresses increased significantly, going from 76.76 to 78.20 MPa range in the healthy tooth to 240.24–243.75 MPa in case of flowable composite. For the resin cement, the maximum von-Mises stress estimated were slightly lower, and had the same magnitude for both the enamel and dentin (218.99 MPa). The resin adhesive generated the lowest stresses at the reattached tooth. The maximum von-Mises stress quantified for resin adhesive was 148.09 MPa for both enamel and dentin.

4. Discussion

Reattachment of fractured teeth fragments is a viable treatment option that conservatively restores esthetics and function [29]. It is associated with short-and medium-term successful outcomes. However, according to Andreasen et al. [30], reattachment failures may occur with new trauma or parafunctional habits. Computational analysis of stresses in a permanent maxillary central incisor tooth, reattached after sustaining a crown-root fracture, has not been reported in the literature so far. This study is the first that aimed to decipher the stress patterns in a reattached and a healthy tooth model, subjected to masticatory load and secondary traumatic loading, using finite element (FE) analysis. The null hypothesis, that the stresses and strains generated during the traumatic loading would not affect the already treated tooth, was rejected. The key highlight was that the stresses generated due to secondary trauma affected the reattached tooth.

Maxillary central incisor tooth being the most frequently affected tooth by TDIs, was chosen for FE modelling [31–33]. According to Stuart et al. [34], the force necessary to cause root fracture must be in the order of 1600 N. Some studies use a force of 800 N to simulate mild traumatic situations, which in most cases result in enamel fractures only [18,23,

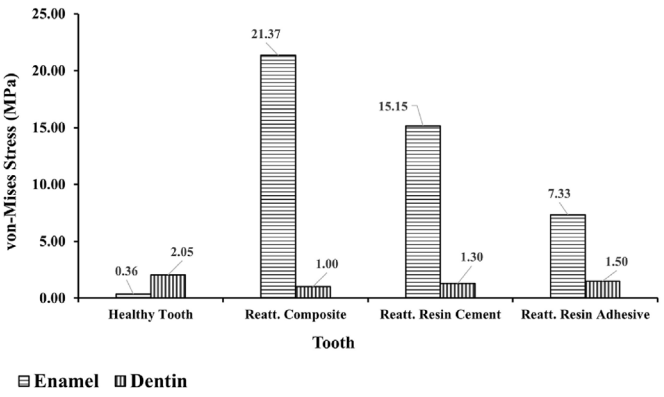

Fig. 9. von-Mises stresses in enamel and dentin due to masticatory load.

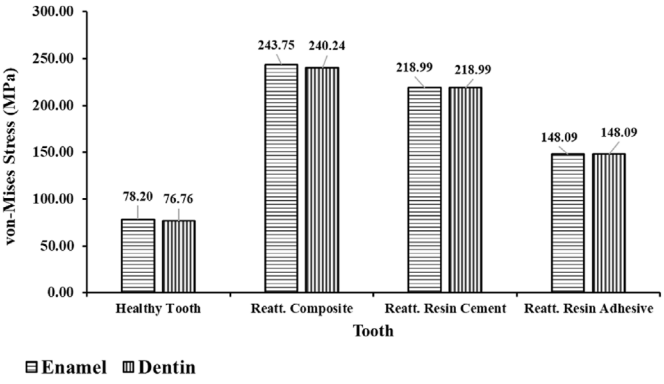

Fig. 10. von-Mises stresses in enamel and dentin at traumatic load.

35]. Based on extensive review of the literature, a pressure equivalent to the force of 2000 N was used to simulate a traumatic load in our analyses.

The results of the present study are clinically relevant since it underscores the fact that the maximum stress as a result of masticatory load on a permanent maxillary central incisor tooth is 2.05 MPa, which is less than the compressive stress limits of enamel (38 MPa) and dentin (163 MPa). Hence, the masticatory load is well tolerated by a healthy maxillary central incisor tooth. Similarly, the maximum shear stress of 1.12 MPa imply that a healthy maxillary central incisor tooth well tolerates the biting forces. However, the stresses due to the same masticatory load in the reattached tooth model were found to be higher. The maximum shear stress generated was 11.92 MPa with flowable composite. Since the shear bond strength of conventional flowable composite is 14.87 $\pm$ 3.4 MPa [36], it can be inferred that the tooth reattached with flowable composite can safely tolerate the masticatory load. However, the maximum stress generated as a result of a traumatic loading was 135.63 MPa, implying that fracture/dislodgement of the fractured segments may occur due to a secondary traumatic event. Similarly, a maximum stress value of 8.31 MPa was observed in the tooth model reattached with resin cement. Since the stress developed is greater than the shear bond strength of resin cement (5.38 MPa) [37], the tooth may not well-tolerate the masticatory load. When a traumatic load was applied to the same reattached tooth model, the maximum shear stress generated was of the order of 119.99 MPa. Hence, a tooth reattached with resin cement may fracture again when met with a new trauma. The maximum stress developed in the tooth model reattached with resin adhesive was 3.92 MPa. Since the shear bond strength of resin adhesive is 24 MPa [38], masticatory loads may be safely tolerated. However, the maximum stress generated was 81.86 MPa in response to the traumatic force which exceeds the shear bond strength of the resin adhesive.

The lowest von-Mises stresses were generated with resin adhesive which was 7 MPa higher than that of the healthy tooth and much lower

than the tensile strength. The stresses developed in the enamel were almost 20 fold more in the reattached tooth with composite. Overall, the maximum shear stresses were generated in the tooth model reattached with flowable composite followed by resin cement. The least amount of stress was observed with resin adhesive. The results of the present study are in accordance with the findings of Farik et al. [39], who have concluded that adhesive with an unfilled resin should be used when restoring fractured teeth by reattachment. Furthermore, maximum shear stresses were concentrated along the fracture line and the CEJ and were quantified to be 11.92 MPa, 8.31 MPa and 3.92 MPa with composite, resin cement and resin adhesive respectively as a result of masticatory load. These stresses increased to 135.63 MPa, 119.99 MPa and 81.86 MPa when a traumatic force was applied. The results are in line with the tensile and compression zones identified when the tooth is subjected to a vertical force [40]. These findings also corroborate with those reported by Chazine et al. [7], where failure occurred at the interface between the tooth and the repair material which was the reattachment line and the weakest point in all the specimens. Similar trend in stress distribution in the cervical region has also been reported due to bruxism [41,42].

The physico-mechanical properties of enamel, including the complex microstructure comprising of crystalline prisms, forms a protective layer covering the tooth [43,44]. As reported by Huang et al. [35], enamel fracture lines develop at stress values of 50 MPa and above. Additionally, dentin possesses a higher deformation capacity until fracture when compared with enamel [45]. These properties enable the tooth to withstand the masticatory load. However, the stresses generated during a traumatic event exceeds the compressive strength (CS) value of 38 MPa for enamel and 163 MPa for dentin and can result in dislodgment/fracture of the reattached coronal fragment from the remaining tooth.

Some of the limitations associated with the current model include assumption of simple loads and boundary conditions. Isotropic linear material properties were considered and some of the biological structures (e.g., gingival tissue and vasculature) were neglected due to lack of data. Although the data was collected from a single patient, it was considered to be translatable across different patients. Despite these limitations, the results of the present study are clinically significant. In future, investigating anisotropic material properties and complex loading scenarios are anticipated to lead to the development of computational models with higher accuracy.

As the focus of this work was to understand the effect of these materials on the traumatic stresses after the re-attachment, the aspect of whether different restoration materials may have different effects on varying ages was not looked upon. Future studies including numerous CBCT scans of different teeth of varying ages, and selection of age-specific restoration materials would further help in enhancing knowledge about the effectiveness of the age-specific adhesive materials for fragment reattachment in traumatic dental fractures. Also, a tooth is generally pulled by applying a rotational motion. The applied rotational force twists the dentin and results in an internal socket expansion. This further leads to tearing of periodontal ligament fibers in teeth with single and conical roots like the maxillary incisors. In addition to this, tractional forces restricts the overall pulling of the tooth. These points have also been explained in a previous work by Jain [46]. Future work studying the effect of different mechanical loads of the tooth after re-attachment could provide insights into better performing materials.

5. Conclusion

The presented computational model showed high differences amongst the selected materials across healthy and a highly common and prominent crown-root fracture affected reattached tooth. The masticatory load was well-tolerated by the reattached tooth post trauma. However, in the event of a second/new trauma, the fracture of the reattached fragments may occur easily. Novel findings of this work showed lowest von-mises and shear stresses in the case of resin adhesive as compared to other materials. Hence, it may be a better option for tooth reattachment over commonly used flowable composite and resin cements. The finite element modelling techniques for common crown-root fractures would be helpful to medical practitioners and manufacturing companies to first test the adhesive materials and then implement based on the lower stress outcomes. Also, for long-term clinical success, the developed computational model can be used to test and fabricate mouth guards for outdoor and sports related activities, and also to provide patient education about trauma prevention and treatments.

Acknowledgment

AK would like to acknowledge the SFRF-2021 Programme of CEP, IIT Delhi. AC and NT would like to acknowledge the funding support by IITD-AIIMS MFIRP Grant, 2022-23.

References

[1] J.O. Andreasen, Etiology and pathogenesis of traumatic dental injuries. A clinical study of 1,298 cases, Scand. J. Dent. Res. 78 (1970) 329–342, https://doi.org/10.1111/J.1600-0722.1970.TB02080.X.
[2] M.D. Turgut, N. Gönül, N. Altay, Multiple complicated crown-root fracture of a permanent incisor, Dent. Traumatol. 20 (2004) 288–292, https://doi.org/10.1111/J.1600-9657.2004.00248.X.
[3] A. Choudhary, R. Garg, A. Bhalla, R. Khatri, Tooth fragment reattachment: an esthetic, biological restoration, J. Nat. Sci. Biol. Med. 6 (2015) 205, https://doi.org/10.4103/0976-9668.149123.
[4] G.V. MacEdo, P.I. Diaz, C.A. Carlos, A.V. Ritter, Reattachment of anterior teeth fragments: a conservative approach, J. Esthetic Restor. Dent. 20 (2008) 5–18, https://doi.org/10.1111/J.1708-8240.2008.00142.X.
[5] F.C.P. Garcia, D.L.N. Poubel, J.C.F. Almeida, I.P. Toledo, W.R. Poi, E.N.S. Guerra, et al., Tooth fragment reattachment techniques-A systematic review, Dent. Traumatol. 34 (2018), https://doi.org/10.1111/EDT.12392.
[6] P. Khandelwal, S. Srinivasan, B. Arul, V. Natanasabapathy, Fragment reattachment after complicated crown-root fractures of anterior teeth: a systematic review, Dent. Traumatol. 37 (2021) 37–52, https://doi.org/10.1111/EDT.12602.
[7] M. Chazine, M. Sedda, H.F. Ounsi, R. Paragliola, M. Ferrari, S. Grandini, Evaluation of the fracture resistance of reattached incisal fragments using different materials and techniques, Dent. Traumatol. 27 (2011) 15–18, https://doi.org/10.1111/J.1600-9657.2010.00951.X.
[8] S. Gupta, G. Singh, A. Chanda, Prediction of diabetic foot ulcer progression: a computational study, Biomed Phys Eng Express 7 (2021), https://doi.org/10.1088/2057-1976/AC29F3.
[9] S. Gupta, V. Gupta, A. Chanda, Biomechanical modeling of novel high expansion auxetic skin grafts, Int j Numer Method Biomed Eng (2022), https://doi.org/10.1002/CNM.3586.
[10] A. Garg, S. Gupta, N. Tewari, S. Srivastav, A. Chanda, Effect of adhesive aterials in Re-attachment of crown and crown–root fractures of permanent maxillary anterior tooth: a computational study, Math. Comput. Appl. 28 (2023) 41, https://doi.org/10.3390/MCA28020041. Page 41 2023;28.
[11] V. Kulkarni, D. Sharma, N. Banda, M. Solanki, V. Khandelwal, P. Airen, Clinical management of a complicated crown-root fracture using autogenous tooth fragment: a biological restorative approach, Contemp. Clin. Dent. 4 (2013) 84, https://doi.org/10.4103/0976-237X.111603.
[12] A. Artieda-Estanga, P. Castelo-Baz, A. Bello-Castro, I. Ramos-Barbosa, B. Martin-Biedma, J. Blanco-Carrion, Management of a crown-root fracture: a novel technique with interdisciplinary approach, J Clin Exp Dent 10 (2018) e620, https://doi.org/10.4317/JCED.54811. –3.
[13] X. Wang, D. Wang, Y rong Wang, X gang Cheng, Ni L. xing, W. Wang, et al., Effect of access cavities on the biomechanics of mandibular molars: a finite element analysis, BMC Oral Health 23 (2023) 1–8, https://doi.org/10.1186/S12903-023-02878-3/FIGURES/3.
[14] D.K. Rathod, C. Chakravarthy, S.S. Suryadevara, R.S. Patil, S.S. Wagdargi, Stress distribution of the zygomatic implants in post-mucormycosis case: a finite element analysis, J. Maxillofac. Oral Surg. 22 (2023) 695–701, https://doi.org/10.1007/S12663-023-01914-7/TABLES/4.
[15] R.S. Sender, D.S. Strait, The biomechanics of tooth strength: testing the utility of simple models for predicting fracture in geometrically complex teeth, J. R. Soc. Interface 20 (2023), https://doi.org/10.1098/RSIF.2023.0195.
[16] M. de P. Rodrigues, P.B.F. Soares, A.D.C.M. Valdivia, R.S. Pessoa, C. Veríssimo, A. Versluis, et al., Patient-specific finite element analysis of fiber post and ferrule design, J. Endod. 43 (2017) 1539–1544, https://doi.org/10.1016/J.JOEN.2017.04.024.
[17] F. Zarone, R. Sorrentino, D. Apicella, B. Valentino, M. Ferrari, R. Aversa, et al., Evaluation of the biomechanical behavior of maxillary central incisors restored by means of endocrowns compared to a natural tooth: a 3D static linear finite elements analysis, Dent. Mater. 22 (2006) 1035–1044, https://doi.org/10.1016/J.DENTAL.2005.11.034.
[18] I.A.V.P. Poiate, A.B. de Vasconcellos, R.B. de Santana, E. Poiate, Three-dimensional stress distribution in the human periodontal ligament in masticatory,

parafunctional, and trauma loads: finite element analysis, J. Periodontol. 80 (2009) 1859–1867, https://doi.org/10.1902/JOP.2009.090220.
[19] P. Linsuwanont, A. Versluis, J.E. Palamara, H.H. Messer, Thermal stimulation causes tooth deformation: a possible alternative to the hydrodynamic theory? Arch. Oral Biol. 53 (2008) 261–272, https://doi.org/10.1016/J.ARCHORALBIO.2007.10.006.
[20] S. Chatterjee, A. Chanda, Development of a tribofidelic human heel surrogate for barefoot slip testing, J Bionic Eng 19 (2022) 429–439, https://doi.org/10.1007/S42235-021-00138-0, 192 2022.
[21] A. Chanda, T. Ruchti, W. Upchurch, Biomechanical modeling of prosthetic mesh and human tissue surrogate interaction, Biomimetics 3 (2018) 27, https://doi.org/10.3390/BIOMIMETICS3030027, 27 2018;3.
[22] Nelson SJ. Wheeler's Dental Anatomy, Physiology, and Occlusion. n.d..
[23] H.M. Huang, C.Y. Tsai, H.F. Lee, C.T. Lin, W.C. Yao, W.T. Chiu, et al., Damping effects on the response of maxillary incisor subjected to a traumatic impact force: a nonlinear finite element analysis, J. Dent. 34 (2006) 261–268, https://doi.org/10.1016/J.JDENT.2005.06.007.
[24] ISO - ISO 4049:2009, Dentistry — polymer-based restorative materials, n.d, https://www.iso.org/standard/42898.html. April 14, 2022).
[25] S. Gupta, A. Chanda, Biomechanical modeling of footwear-fluid-floor interaction during slips, J. Biomech. 156 (2023) 111690, https://doi.org/10.1016/J.JBIOMECH.2023.111690.
[26] S. Gupta, S. Chatterjee, A. Chanda, Influence of vertically treaded outsoles on interfacial fluid pressure, mass flow rate, and shoe–floor traction during slips, Fluid 8 (2023) 82, https://doi.org/10.3390/FLUIDS8030082, 82 2023;8.
[27] S. Gupta, S. Chatterjee, A. Malviya, G. Singh, A. Chanda, A novel computational model for traction performance characterization of footwear outsoles with horizontal tread channels, Comput. Times 11 (2023) 23, https://doi.org/10.3390/COMPUTATION11020023. Page 23 2023;11.
[28] Y. Nyashin, Biomechanical Modelling of Periodontal Ligament Behaviour under Various Mechanical Loads - Acta of Bioengineering and Biomechanics - Tom, vol. 2, Biblioteka Nauki - Yadda, 2000 nr 2 (2000).
[29] G. Rappelli, C. Massaccesi, A. Putignano, Clinical procedures for the immediate reattachment of a tooth fragment, Dent. Traumatol. 18 (2002) 281–284, https://doi.org/10.1034/J.1600-9657.2002.00099.X.
[30] F.M. Andreasen, J.G. Norén, J.O. Andreasen, S. Engelhardtsen, U. Lindh-Strömberg, Long-term survival of fragment bonding in the treatment of fractured crowns: a multicenter clinical study, Quintessence Int. 26 (1995) 669–681.
[31] E.B. Bastone, T.J. Freer, J.R. McNamara, Epidemiology of dental trauma: a review of the literature, Aust. Dent. J. 45 (2000) 2–9, https://doi.org/10.1111/J.1834-7819.2000.TB00234.X.
[32] T.L. Ravishankar, M.A. Kumar, N. Ramesh, T.R. Chaitra, Prevalence of traumatic dental injuries to permanent incisors among 12-year-old school children in Davangere, South India, Chin. J. Dent. Res. 13 (2010) 57–60.
[33] C. Stewart, M. Kinirons, P. Delaney, Clinical audit of children with permanent tooth injuries treated at a dental hospital in Ireland, Eur. Arch. Paediatr. Dent. 12 (2011) 41–45, https://doi.org/10.1007/BF03262778.
[34] C.H. Stuart, S.A. Schwartz, T.J. Beeson, Reinforcement of immature roots with a new resin filling material, J. Endod. 32 (2006) 350–353, https://doi.org/10.1016/J.JOEN.2005.08.001.
[35] H.M. Huang, K.L. Ou, W.N. Wang, W.T. Chiu, C.T. Lin, S.Y. Lee, Dynamic finite element analysis of the human maxillary incisor under impact loading in various directions, J. Endod. 31 (2005) 723–727, https://doi.org/10.1097/01.DON.0000157992.29221.41.
[36] K. Poorzandpoush, M. Shahrabi, A. Heidari, Z.S. Hosseinipour, Shear bond strength of self-adhesive flowable composite, conventional flowable composite and resin-modified glass ionomer cement to primary dentin, Front Dent 16 (2019) 62–68, https://doi.org/10.18502/FID.V16I1.1111.
[37] M.P. Sethusa, A.K. Seedat, I.C. du Preez, P. Hlongwa, Shear bond strength comparison of RelyX Unicem with six other orthodontic resin adhesive systems, SADJ 64 (2009) 72–75.
[38] K. Navyasri, R.K. Alla, G. Vineeth, S.S. Mc, An overview of dentin bonding agents, Int J Dent Mater 1 (2019) 60–67, https://doi.org/10.37983/IJDM.2019.1204.
[39] B. Farik, E.C. Munksgaard, J.O. Andreasen, S. Kreiborg, Fractured teeth bonded with dentin adhesives with and without unfilled resin, Dent. Traumatol. 18 (2002) 66–69, https://doi.org/10.1034/J.1600-9657.2002.180203.X.
[40] B.R. da Silva, Moreira Neto Jjs, F.I. da Silva, A.S.W. de Aguiar, Finite element analysis applied to dentoalveolar trauma: methodology description, ISRN Dent 2011 (2011) 1–5, https://doi.org/10.5402/2011/297132.
[41] B. Dejak, A. Młotkowski, Finite element analysis of strength and adhesion of cast posts compared to glass fiber-reinforced composite resin posts in anterior teeth, J. Prosthet. Dent 105 (2011) 115–126, https://doi.org/10.1016/S0022-3913(11)60011-5.
[42] E.B. de Las Casas, T.P.M. Cornacchia, P.H. Gouvêa, C.A. Cimini, Abfraction and anisotropy–effects of prism orientation on stress distribution, Comput. Methods Biomech. Biomed. Eng. 6 (2003) 65–73, https://doi.org/10.1080/1025584021000043357.
[43] N.J. Cochrane, F. Cai, N.L. Huq, M.F. Burrow, E.C. Reynolds, New approaches to enhanced remineralization of tooth enamel, J. Dent. Res. 89 (2010) 1187–1197, https://doi.org/10.1177/0022034510376046.
[44] M. Baldassarri, H.C. Margolis, E. Beniash, Compositional determinants of mechanical properties of enamel, J. Dent. Res. 87 (2008) 645–649, https://doi.org/10.1177/154405910808700711.
[45] S. Poolthong, T. Mori, M.V. Swain, Determination of elastic modulus of dentin by small spherical diamond indenters, Dent. Mater. J. 20 (2001) 227–236, https://doi.org/10.4012/DMJ.20.227.
[46] A. Jain, Principles and techniques of exodontia, Oral Maxillofac. Surg. Clin. (2021) 259–297, https://doi.org/10.1007/978-981-15-1346-6_13/FIGURES/39.